Journal of Cleaner Production 272 (2020) 122764

Contents lists available at ScienceDirect

Journal of Cleaner Production

journal homepage: www.elsevier.com/locate/jclepro

Efficient selection of conventional and phase-change CO_2 capture solvents and mixtures based on process economic and operating criteria

Theodoros Zarogiannis [a, b], Athanasios I. Papadopoulos [a, *], Panos Seferlis [a, b]

[a] Chemical Process and Energy Resources Institute, Centre for Research and Technology-Hellas, Thermi, 57001, Thessaloniki, Greece
[b] Department of Mechanical Engineering, Aristotle University of Thessaloniki, 54124, Thessaloniki, Greece

ARTICLE INFO

Article history:
Received 26 July 2019
Received in revised form
3 June 2020
Accepted 9 June 2020
Available online 9 July 2020

Handling editor: Yutao Wang

Keywords:
CO_2 capture
Phase-change solvents
Mixtures
Economic assessment
Shortcut models
Energy reduction

ABSTRACT

The aim of this work is to exploit shortcut models in order to efficiently assess conventional and phase-change solvents and mixtures based on CO_2 capture and upstream plant process and economic performance criteria. This is approached by exploiting a previously available shortcut model which is currently suitable only for solvents exhibiting vapor-liquid equilibrium (VLE) behavior. This model is extended to account for solvents which exhibit vapor-liquid-liquid equilibrium (VLLE), phase-change behavior and is implemented in 10 solvents and mixtures, including 2 phase-change solvents. The VLE behavior of conventional solvents and mixtures is represented using models obtained from literature or regressed from experimental data. The VLLE behavior of the phase-change solvents MAPA/DEEA (3-(methylamino) propylamine/2-(diethylamino)ethanol) and MCA (methyl-cyclohexylamine) is modelled through regression curves from experimental data. The performance criteria for solvent assessment include cyclic capacity, solvent flowrate and purchase cost, regeneration duty, net efficiency penalty and lost revenue of power plant from parasitic electricity due to capture. The performance of the phase-change solvents is validated based on literature data, whereas it is superior to that of conventional CO_2 capture solvents. The net efficiency penalties of MCA and MAPA/DEEA are approximately between 2.9 and 3.3% points lower than MEA (monoethanolamine), whereas the lost revenue of the power plant due to the capture unit is 47% and 50% lower than MEA, respectively.

1. Introduction

Chemical absorption has received significant attention as a promising technology for post combustion CO_2 capture (Bui at el., 2018). It is a well-established process, it can be easily adapted in existing plants and the required conditions for CO_2 capture are easy to satisfy. However, a main drawback is the large energy requirement for solvent regeneration. To this end, numerous articles have been published in order to address this downside, focusing on the development of new solvents and of improved process systems to reduce the associated capital and operating costs (overview in Papadopoulos and Seferlis, 2017a,b; Bui at el., 2018). In recent years, such innovations are increasingly sought through model-based approaches. The vast majority of existing works employs rigorous process flowsheet models (Papadopoulos and Seferlis, 2017a,b) which include equilibrium or non-equilibrium representations of the underlying chemical and physical phenomena (e.g., mass transfer, reaction kinetics and so forth). This is clearly useful, but their development often requires intense human effort. Computational intensity is also significant due to the use of non-linear, algebraic or differential-algebraic models. Such challenges limit the evaluation approaches of solvents to the use of simpler indicators such as capture loadings and rarely reboiler duty, instead of the desired capture process and upstream plant economics.

On the other hand, shortcut models are easy to develop and computationally efficient. They can be used for simulation of CO_2 capture systems, provided that they can be sufficiently enhanced to account for the non-ideal behavior of the solvent-water-CO_2 mixtures. In this context, they have been implemented in few occasions in CO_2 capture research. Notz et al. (2011) propose an equilibrium stage model using a modified Kremser equation (Kremser, 1930). It is used for the calculation of the absorption/desorption process

* Corresponding author.
E-mail address: spapadopoulos@certh.gr (A.I. Papadopoulos).

https://doi.org/10.1016/j.jclepro.2020.122764
0959-6526/

reboiler duty, providing also information regarding the number of stages in the two columns. The model accounts for the non-linear equilibrium line through necessary linearizations. The method provides good matching of the experimental data and is implemented for MEA (Monoethanolamine). A typical Kremser model is used in Tock and Maréchal (2014) in order to determine the cost of a CO_2 capture process. The work aims to produce cost and energy correlations for CO_2 capture systems, which can be used in optimization. The employed solvent is MEA. A shortcut model for the calculation of the reboiler duty is also proposed by Rochelle et al. (2011). This process employs 40 wt% PZ (Piperazine) with regeneration represented by a two-stage flash without considering a stripper. A shortcut method is used by Reddick et al. (2014) for the optimization of a post-combustion CO_2 capture process enhanced with ejectors for waste heat upgrading. This study investigates the impact of the placement of steam injection into the stripper tower, the CO_2 loading of the solvent entering the reboiler from the stripper, the stripper pressure, and the source of the secondary ejector steam. The model accounts for the non-ideal phase behavior of MEA−H_2O−CO_2 and is also used to evaluate the number of stages of the stripper. A shortcut model based on the shortest stripping line distance approach is proposed by Lucia et al. (2010) for the determination of the minimum regeneration energy of the post combustion CO_2 capture process. The authors also consider MEA as the solvent. Finally, Kim et al. (2015) propose a shortcut estimation method which focuses on the intermediate heat exchange and desorption part of the process, while accounting entirely for the non-ideal phase-change behavior of the solvent in the presence of water and CO_2. Reported applications include the simulation of MEA and PZ. The authors don't consider the number of stages of either column in the proposed model. Sizing of the columns is clearly very important, but the model can still provide significant operating information including the necessary solvent flowrate, rich and lean stream loadings, temperature information in the desorber as well as reboiler duties. Such information is sufficient for solvent screening purposes as it directly incorporates operating expenses in solvent selection, while the model is computationally very efficient.

Apparently, existing shortcut models have been used only for MEA and PZ. There are numerous other solvents and mixtures that are worth of investigation in terms of process economic and operating performance. In recent years the focus is shifting toward the so-called phase-change solvents (Papadopoulos et al., 2019) that require regeneration energy in the range of 2.0−2.5 GJ/ton of CO_2 captured, which is much lower than the 4.0 GJ/ton CO_2 reported for MEA. Such solvents include amines that exhibit liquid-liquid phase separation upon a change in processing conditions. The liquid-liquid phase-change enables non-thermal separation of a CO_2-lean phase which is recycled to the absorber prior to desorption. This reduces the flow of material that enters the desorber for regeneration, while desorption may take place at much lower temperature than with conventional solvents.

Existing works that address the simulation of phase-change solvents include those of Tan (2010), Zhang et al. (2011) and Zhang (2014) for few options of the thermomorphic, biphasic solvent family, of Raynal et al. (2011a,b; 2014), Gomez et al. (2014), Dreillard et al. (2017) for the DMX solvent and Liebenthal et al. (2013) for MAPA/DEEA (3-(methylamino)propylamine/2-(diethylamino)ethanol). These works largely employ in-house or commercial process simulators with the aim to evaluate process economics of the particular solvents at hand, providing few details regarding the employed model features. Such solvents are expected to exhibit more intense computational challenges than conventional solvents, due to the additional appearance of the liquid-liquid phase separation. Shortcut models could be very useful, but they cannot be used in their current form as they do not account for liquid-liquid phase-change. Economic or operating performance details are available only for DMX and MAPA/DEEA. For all other phase-change solvents information is available only for the capture loadings and in few occasions for the reboiler duty (Papadopoulos et al., 2019). This is due to the scarcity of thermodynamic data and the difficulties in developing the process models required to calculate economic indicators. The same holds for numerous, non-phase-change solvents and especially mixtures.

In this work we propose a novel shortcut model in order to efficiently assess phase-change solvents by extending the model of Kim et al. (2015). The latter is also used for the first time as a shortcut model for conventional solvents and mixtures other than MEA and PZ. We further evaluate for the first time the performance of 10 solvents and mixtures, including 2 phase-change solvents, based on several capture and upstream plant process and economic performance criteria. The latter include cyclic capacity, solvent flowrate and purchase cost, regeneration duty, net efficiency penalty and lost revenue from parasitic electricity due to capture. Such indicators are very important. To develop the necessary models, we derive thermodynamic relationships of partial CO_2 pressure and enthalpy as functions of loadings and temperature using the gSAFT (2018) software, as well as other experimental sources for solvents and mixtures. We further derive simple correlations to calculate net efficiency penalty and lost revenue from parasitic losses.

2. Models and methods

2.1. Overview of model for solvents exhibiting VLE

Fig. 1 shows a flowsheet of a regular absorption-desorption CO_2 capture process. It consists of an absorber, a stripper, a heat exchanger a reboiler and pumps for the recirculation of the solvent. The flue gas contains the CO_2 which enters the absorber. The aqueous solvent solution enters at the absorber top and the absorber outlet at stream 1 consists of the CO_2-amine product and water. Stream 1 enters the heat exchanger where it is heated. Stream 5 exits the heat exchanger and enters the stripper. It is rich in CO_2 and in equilibrium with the vapor phase. Stream 6 exits the reboiler. It is lean in CO_2 due to the regeneration energy given to the reboiler which has been used to separate part of the CO_2 in the stripper. It then enters the heat exchanger, transferring heat to stream 1.

The calculation of the regeneration energy using the model proposed by Kim et al. (2015) requires the determination of two, separate operating regions for the implementation of the necessary energy balance. The latter is focused around the heat exchanger (HX) for Region A (streams 1, 2, 5, 6) and around the reboiler for Region B (streams 6, 7, 8). The region boundaries are determined by the value of the lean loading. Kim et al. (2015) observe that region A corresponds to column operation at high lean loading values (e.g., higher than 0.2 mol CO_2/mol amine for MEA). In region A, the flow rate and enthalpy of stream 5 dominate those of the other incoming streams to the top stage (condensed water and upward vapor from the lower stages). Region B corresponds to operation at lower lean loading values. In this case a larger amount of thermal energy is provided to the reboiler to separate CO_2 by increasing the reboiler temperature. The upward vapor stream 8 has a stronger effect on the top stage than in region A.

For region A, the overall energy balance of the stripper can be described by the following relationship:

$$F_1 \cdot H_1 + F_4 \cdot H_4 + Q_{regen} - F_2 \cdot H_2 - F_3 \cdot H_3 = 0 \quad (1)$$

Based on the above equation, the shortcut method of Kim et al.

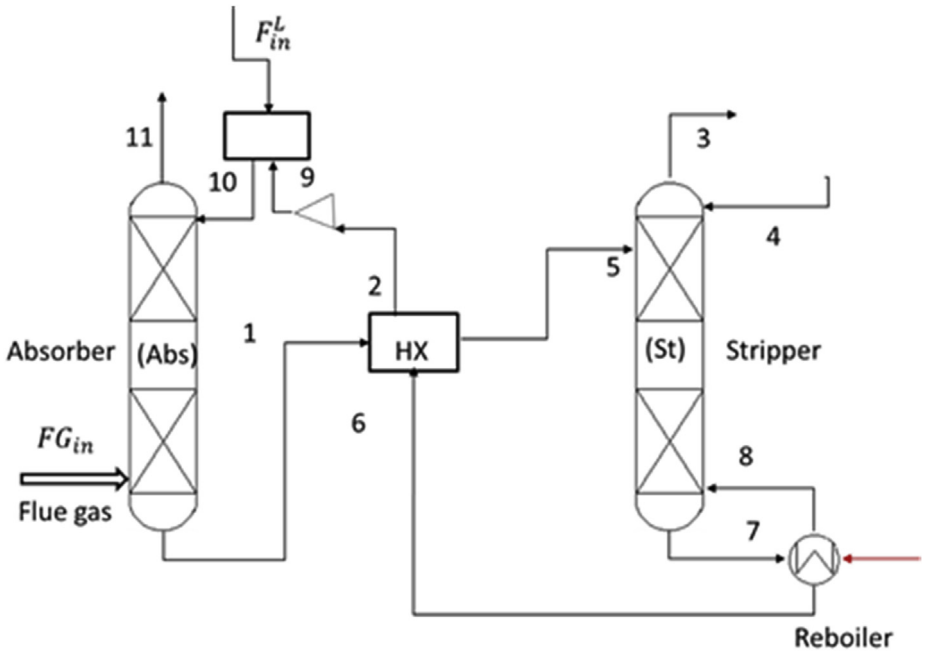

Fig. 1. Typical flowsheet of the chemical absorption – desorption process for CO_2 capture.

(2015) calculates the regeneration energy together with other important process parameters. The regeneration energy Q_{regen} can be estimated through Eq. (2) from the energy terms of the sensible heat Q_{sens}, the latent heat Q_{latent} and the heat of reaction Q_{rxn} needed for the breakage of the CO_2-amine bond.

$$Q_{regen} = Q_{sens} + Q_{latent} + Q_{rxn} \quad (2)$$

For region B, Q_{regen} is determined through Eq. (3) based on an energy balance implemented around the reboiler (Fig. 2).

$$Q_{regen} = -m_{am}H_6 - m_8H_8 + m_{am}H_7 \quad (3)$$

Details and modeling equations for regions A and B are reported in the Supporting Information.

2.2. Model for solvents exhibiting VLLE

2.2.1. Main concepts

Phase-change solvents are characterized by the presence of Vapor-Liquid-Liquid equilibrium where one liquid phase is rich in

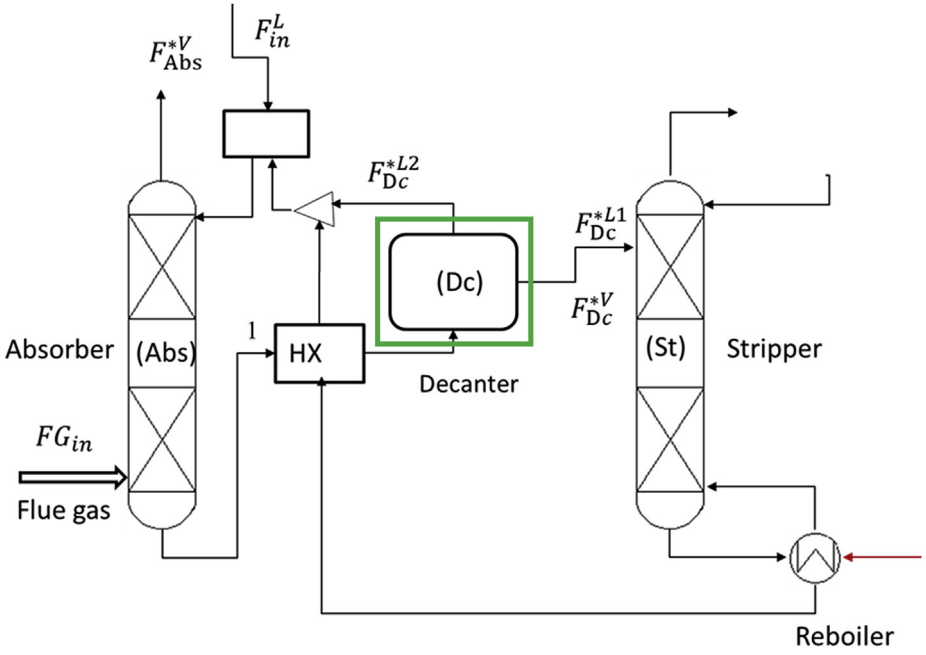

Fig. 2. Typical diagram of the chemical absorption – desorption process for CO_2 capture using PC1 (MCA).

CO_2, while the other phase is lean in CO_2 and rich in amine. Liquid-liquid phase separation temperature (LLPS) is a key parameter and very important from a process perspective because it determines the placement of the mechanical separator and the number of phases present in the absorber (Zhang, 2014). Based on the LLPS there are currently two main classes of phase-change solvents; ones that exhibit phase-separation at absorption column conditions (e.g., 40 °C) and ones that exhibit phase-change at higher temperatures. Table 1 summarizes the characteristics of one representative from each class, namely MAPA/DEEA and MCA. The phase-change behavior and process performance are well documented in published literature for MAPA/DEEA (Pinto et al., 2014a,b; Arshad, 2014) while data which enable the process assessment of MCA are also available (Zhang, 2014; Tzirakis et al., 2019a). Note that equilibrium data for phase-change solvents are scarce, hence the availability of three-phase data for these two solvents is the main reason for their selection.

MCA is a member of the lipophilic amines family of phase-change solvents; in such solvents the liquid-liquid phase split appears after reaction with CO_2 and heating (Zhang, 2014). They are characterized by high cyclic loading capacity and low regeneration temperature in the range of 60°C–90 °C which reduces the required reboiler heat. As shown in Table 1 and Fig. 2, MCA is characterized by the placement of the liquid-liquid phase separator after the intermediate heat exchanger (HX) in the absorption/desorption flowsheet, assuming that there is a single phase of liquid inside the absorber.

In the case of aqueous MAPA/DEEA solutions, two liquid phases appear at 40 °C upon reaction with CO_2, (Pinto et al., 2014a). MAPA and water are found mainly in the heavy, CO_2-rich phase, while DEEA is found in the light, CO_2-lean phase. Only the CO_2-rich phase needs to be regenerated rendering this mixture a potential solvent system with low regeneration heat requirement in the stripper (2.2–2.5GJ/ton CO_2). This mixture combines the best properties of both amines, i.e. the high absorption capacity of DEEA and the fast reaction kinetics of MAPA (Arshad, 2014). MAPA/DEEA requires a liquid-liquid phase separator before the intermediate HX (Fig. 3).

2.2.2. Model development

A typical flow diagram of a phase-change process for PC1 solvent types (e.g. MCA) is shown in Fig. 2. The CO_2-lean phase is recycled to the absorber and the CO_2-rich phase is sent to a steam stripping column (Zhang, 2014).

The equations used for the determination of a short-cut model for a phase-change solvent such as MCA are similar to the ones for the model for two phase systems, with the addition of the equations required to calculate the liquid-liquid split in the decanter. The aim is to calculate the mass flowrate that enters the desorber after the decanter, in order to perform energy balance calculations using the equations reported in the Supporting Information. This is determined through Eqs. (4)–(7) that describe the overall and component mass balance, as well as the equilibrium relations.

$$F_1 = F_{Dc}^{*L_1} + F_{Dc}^{*L_2} + F_{Dc}^{*V} \tag{4}$$

$$F_1 \cdot x_{1,i} + F_1 \cdot y_{1,i} = F_{Dc}^{*L_1} \cdot x_{Dc,i}^{*L_1} + F_{Dc}^{*L_2} \cdot x_{Dc,i}^{*L_2} + F_{Dc}^{*V} \cdot y_{Dc,i}^{*} \tag{5}$$

$$y_{Dc,i}^{*} = K_{Dc,i} \cdot x_{Dc,i}^{*L_1} \tag{6}$$

$$x_{Dc,i}^{*L_1} = K_{Dc,i}^{'} \cdot x_{Dc,i}^{*L_2}, \forall i \in \{CO_2,\ H_2O,\ PC1\} \tag{7}$$

The star indicates that the balance equations correspond to equilibrium data at the desired absorption and liquid-liquid separation temperatures and pressures, for known flue gas and solvent input streams. Stream $F_{Dc}^{*L_1}$ is used in the calculations of the energy balance models reported in the Supporting Information for the determination of the m_{am}.

Regarding PC2 type solvents (e.g., MAPA/DEEA) the stream from the absorber separates into two phases after absorption (Fig. 3): one CO_2-lean and one CO_2-rich phase (upper and lower phases, respectively). By splitting the two phases in the decanter, the rich phase is sent to the thermal stripper, first passing through the heat exchanger. It then flows from the top of the stripper. After desorption, the regenerated solvent from the stripper enters the absorber together with the lean phase from the decanter (Zhang, 2014).

Using Eqs. (8)–(11) for PC2 type solvents it is possible to determine the two liquid phases that separate immediately after the absorber, since the phase-separation takes place at T_{Abs}. Hence only the lower phase flows into the stripper and the reboiler.

$$F_1 = F_{Dc}^{*L_1} + F_{Dc}^{*L_2} + F_{Dc}^{*V} \tag{8}$$

$$F_1 \cdot x_{1,i} + F_1 \cdot y_{1,i} = F_{Dc}^{*L_1} \cdot x_{Dc,i}^{*L_1} + F_{Dc}^{*L_2} \cdot x_{Dc,i}^{*L_2} + F_{Dc}^{*V} \cdot y_{Dc,i}^{*} \tag{9}$$

$$y_{Dc,i}^{*} = K_{Dc,i} \cdot x_{Dc,i}^{*L_1} \tag{10}$$

$$x_{Dc,i}^{*L_1} = K_{Dc,i}^{'} \cdot x_{Dc,i}^{*L_2}, \forall i \in \{CO_2,\ H_2O,\ PC2\} \tag{11}$$

3. Implementation

3.1. Components and equilibrium models

This work considers both single and mixed amines. A series of non-phase-change amines are compared with phase-change amines. The former represents widely investigated, and often highly performing, CO_2 capture solvents in published literature. They are considered here as reference solvents in order to investigate performance improvements obtained from phase-change solvents. Table 2 shows the short names and molecular structures of the 5 employed single solvents. Table 3 shows the 5 mixed solvents.

In all solvents, the determination of equilibrium CO_2 vapor pressure $P_{CO_2}^{*}$ is needed for the implementation of the shortcut model. $P_{CO_2}^{*}$ is represented by the empirical expression of Oyenekan

Table 1
Main process-related features for the phase-change solvents MCA and MAPA/DEEA.

A/A	Solvent mixture	LLPS	Placement of phase separator	Desorption conditions
PC1	MCA (35%wt.)	above 60 °C	*After* intermediate HEX	90 °C, depending on the separation method (Zhang et al., 2013)
PC2	MAPA/DEEA (2M,5M)	40 °C	*Before* intermediate HEX	100°C–120 °C on average (Pinto et al., 2014a,b)

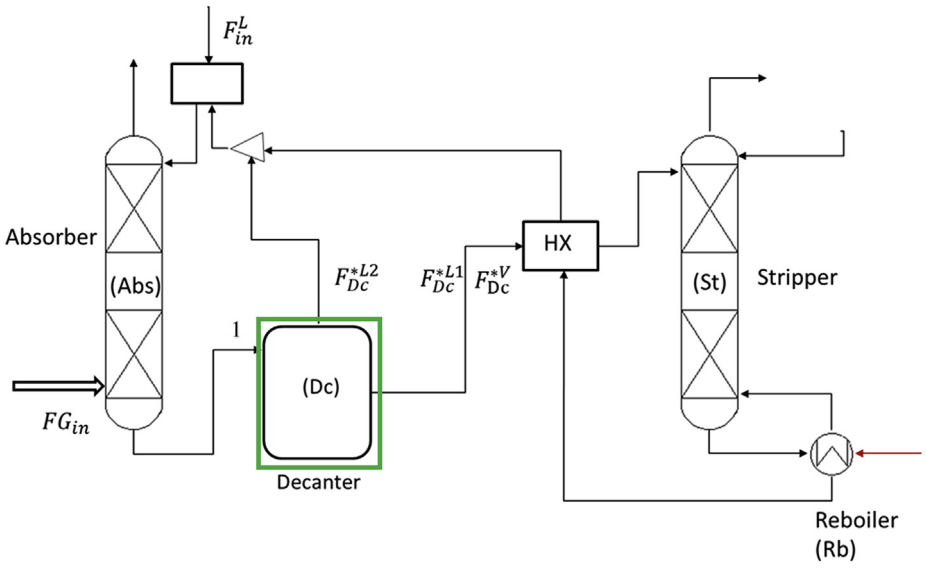

Fig. 3. Typical diagram of the chemical absorption – desorption process for CO_2 capture using PC2 (MAPA/DEEA).

Table 2
List of single solvents.

ID	Short name	Molecular Structure
S1	MEA	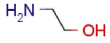
S2	AMP	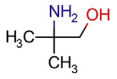
S3	DEA	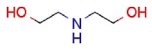
S4	MAPA	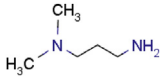
PC1	MCA	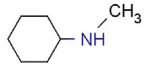

(2007) for all solvents, apart from S2 and MR4:

$$\ln P_{CO_2}^{*} = n + ba + \frac{c}{T} + d\frac{a^2}{T^2} + e\frac{a}{T^2} + f\frac{a}{T} \quad (12)$$

where a stands for the equilibrium CO_2 loading and T for temperature (K). The adjustable constants n, b, c, d, e, and f are taken from Oyenekan (2007) for MEA. They are derived from VLE calculations for the rest of the solvents, using the sources reported in Table 4. The heat of desorption is calculated by differentiating the VLE expression, yielding Eq. (13):

$$-\frac{\Delta H}{R} = c + 2d\frac{a^2}{T} + 2e\frac{a}{T} + (fa) \quad (13)$$

It should be noted that model I for MAPA/DEEA (Table 4) is used for calculations through equations (12) and (13) of the heat of reaction and mass flows other than the second liquid phase that enters the desorber. This is reasonable because the experimental data used to derive model I include operating conditions that account for the reaction of the solvent mixture with CO_2. A second model, namely Model II, is used for calculations related to the mass flow of the second liquid phase, where it is only necessary to use equation (12). Experimental data used for this model focus on the equilibrium behavior of the second liquid phase only, which is of interest in this process model. Numerical details for model II are provided in Table S2 of the Supporting Information, to maintain the clarity of Table 4. The experimental data used to derive model II are from Pinto et al. (2014b), with more details available in Table S7 of the Supporting Information regarding its goodness of fit.

Regarding AMP (S2) and AMP/PZ (MR4), the CO_2 vapor pressure is determined through a polynomial obtained from Oexman (2011) according to Eq. (14). The heat of desorption is calculated by differentiating the VLE expression, producing Eq. (15) as proposed by Oexman (2011).

$$\ln P_{CO_2}^{*} = n + \frac{b}{T} + ca + d\frac{a}{T} + ea^2 + f\frac{a^2}{T} + ga^3 + h\frac{a^3}{T} + ia^4 \quad (14)$$

Table 3
List of mixtures.

Mixture	Component 1	Component 2
MR1	MEA 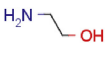	MDEA 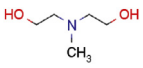
MR2	MPA 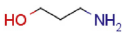	MDEA 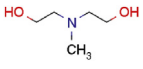
MR3	DEA 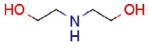	MDEA 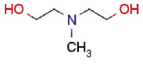
MR4	AMP 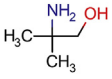	PZ 
PC2	DEEA 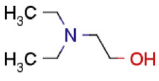	MAPA 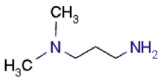

Table 4
Single and mixed solvents constants for the determination of $P^*_{CO_2}$

ID	MEA	DEA	MAPA	MCA
Composition (w/w%)	30	40	18	37.7
a_{rich}	0.47	0.42	1.09	0.629
a_{lean}	0.2	0.05	0.2	0.16
n	35.11	33.68	46.42	50.91
b	−45.04	−46.07	−35.44	−9.33
c	−14281	−12490	−19810	−1.743e+04
d	−546277	−1603000	−354300	−2.685e+05
e	−3400441	−84270	−1301000	5.645e+06
f	32670.01	23430	21630	−1.11e+04
Data source	Oyenekan (2007)	gSAFT (2018) - SAFT-VR SW	Arshad (2014)	Tzirakis et al. (2019a)
Total pressure range (bar)	[1,2]	[1,2]	[1,2]	[1]
$P^*_{CO_2}$ **model**	Eq. (12)	Eq. (12)	Eq. (12)	Eq. (12)
ΔH **model**	Eq. (13)	Eq. (13)	Eq. (13)	Eq. (13)
ID	**MEA/MDEA**	**DEA/MDEA**	**MPA/MDEA**	**MAPA/DEEA** (model I)
Composition (w/w%)	38.6 (1:2)	43.4 (1:2)	40.7 (1:2)	63.5/19.1
a_{rich}	0.32	0.38	0.4847	0.87
a_{lean}	0.2	0.2	0.2	0.19
n	33.76	−0.509	61.38	36.83
b	170.8	164.6	−126.4	−152.9
c	−1.288e+04	−530.3	−2.309e+04	−1.42e+04
d	−4.462e+06	−7.082e+05	−2.775e+06	−2.738e+06
e	3.123e+07	1.456e+07	−2.666e+06	−1.343e+07
f	−1.37e+05	−9.295e+04	6.223e+04	1.031e+05
Data source	gSAFT (2018) - SAFT-VR SW	gSAFT (2018)- SAFT-VR SW	gSAFT (2018)- SAFT-γ Mie EoS	Arshad (2014)
Total pressure range (bar)	[1,2]	[1,2]	[1,2]	[1,2]
$P^*_{CO_2}$ **model**	Eq. (12)	Eq. (12)	Eq. (12)	Eq. (12)
ΔH **model**	Eq. (13)	Eq. (13)	Eq. (13)	Eq. (13)

Table 5
Solvent constants for the determination of $P^*_{CO_2}$

ID	AMP	AMP/PZ
Composition (w/w%)	30	27/13
a_{rich}	0.46	0.69
a_{lean}	0.05	0.43
n	29.28	−9.956
b	−8610	−3146
c	41.03	177.7
d	−4457	−9482
e	−80.68	−322.7
f	9094	−1323
g	52.32	310.6
h	763.2	8040
i	−18.88	−122.5
Data source	Oexman (2011)	Oexman (2011)
Total pressure range (bar)	[1,2]	[1,2]
$P^*_{CO_2}$ **model**	Eq. (14)	Eq. (14)
ΔH **model**	Eq. (15)	Eq. (15)

$$-\frac{\Delta H}{R} = b + da + fa^2 + ha^3 \tag{15}$$

Models (12)–(15) are proposed here as they enable a uniform way of representing phase equilibrium and facilitate the implementation of the shortcut models. They provide valid predictions as shown by the data regarding the goodness of fit reported in the Supporting Information. Different equilibrium models could be used as well. For example, the models of Bruder et al. (2011, 2012) for AMP, AMP/PZ and MAPA could also be used. Loading, a_{rich} is given in Table 4. It is obtained from the VLE data taken from the corresponding data sources at 313 K for $P^*_{CO_2}$ at 10 kPa. a_{rich} for solvents in Table 5 is obtained directly from Oexman (2011).

In some solvents of Table 4 the equilibrium is calculated using gSAFT (2018). This software employs two thermodynamic models which are based on the statistical associating fluid theory (SAFT) (Chapman et al., 1989, 1990). The first model is the SAFT-VR equation of state (Gil-Villegas et al., 1997), which has been used successfully for modeling of several amine-water-CO_2 mixtures with necessary parameters available in Mac Dowell et al. (2009) and Rodriguez et al. (2012). The second model is the SAFT-γ Mie equation of state (Papaioannou et al., 2014; Dufal et al., 2015) which is based on the group contribution concept (Achenie et al., 2002; Papadopoulos et al., 2018). Parameters necessary for predictions using SAFT-γ Mie can be found in Dufal et al. (2014) and Papaioannou et al. (2016). Such SAFT-based methods have been used successfully before by Chremos et al. (2016) and Perdomo et al. (2019) to model the absorption of CO_2 in aqueous alkanolamine solutions presenting a powerful tool to model such complex reactive systems.

Vapor-liquid-liquid equilibrium data for MCA are obtained from experiments by Tzirakis et al. (2019a,b). Vapor phase water data are calculated based on Raoult's law in the VLLE relationships of section 2.2.2. In this case, at 90 °C the $P^*_{CO_2}$ accounts for the rich CO_2, liquid phase entering the desorber. At this temperature, m_{am} (see Supporting Information) represents the CO_2-rich phase that enters the desorber. In the case of MAPA/DEEA the CO_2-rich phase moves into the desorber after passing through the heat exchanger.

Loadings a_{rich} and a_{lean} used in the energy balances (see Supporting Information) correspond to the CO_2 content of the liquid phase entering the desorber. The flue gas consists of N_2 and CO_2 (15 wt%) at a temperature $T_1 = 313$ K with a flow rate 17.1 kmol/h. The operating pressure of the absorber is determined at 1 bar and 1.5 bar in the desorber. The only exception is MCA where the desorber pressure is considered 1 bar, due to availability of data only at this pressure. For the solvents of Tables 4 and 5, the reported a_{lean} are obtained so that T_6 is similar to the T_6 of MEA for all solvents at the corresponding desorber pressure. This is done in order to be able to compare the performance of the solvents starting from the same operating points. The only exception is MCA, where T_6 is 90 °C based on Zhang (2014). The overall CO_2 capture efficiency is considered 90%. The minimum temperature difference ΔT_{MTD} is 10 °C.

Table 6
Amine solvents and their cost (Chem-Space, 2018).

ID	C_{sol}($/gr)
MEA	0.02
AMP	0.04
DEA	0.03
MAPA	0.17
MCA	0.35
MAPA/DEEA	0.062
MEA/MDEA	0.052
MPA/MDEA	0.065
MDEA/DEA	0.052
AMP/PZ	0.049

3.2. Technoeconomic data and models

The solvent performance is assessed using numerous criteria pertaining to CO_2 capture plant process performance as well as the effect that this plant has when it is integrated in a power plant. Heat integration is not considered in the latter case. The employed criteria include regeneration duty (Q_{regen}), cyclic capacity (Δa) defined as the difference between the loading of the rich CO_2 stream at the bottom of the absorber and the loading of the lean stream at the bottom of the stripper, solvent flowrate (m_{am}), net efficiency penalty (*NEP*) defined as the decrease in the net efficiency of the power plant due to the amount of extracted steam at the required pressure for CO_2 capture, solvent purchase cost (C_{sol}), and lost revenue from parasitic electricity due to capture (R_{lost}). The latter represents the equivalent power that is used for capture purposes, instead of being sold to the market. It is desired to have solvents which exhibit maximum Δa values and minimum values in all other indices. C_{sol} is indicative according to Table 6. In case of mixtures the price used in the elaboration of the results is adjusted based on the concentration of solvents.

NEP is a more inclusive index than the reboiler duty, as it additionally accounts for reboiler temperature ($T_{reboiler}$) and desorber pressure (P_{Des}). Reboiler temperature is indicative of the quality of the hot stream necessary to provide the required energy. Desorber pressure accounts for the additional cost of maintaining the desorber at a specific pressure. *NEP* is calculated through a polynomial which is fitted (Table 7) from data extracted from nomograms presented in Oexman (2011), as follows:

$$NEP_{P_{Des}=1.5bar} = p_0 + p_1 \times T_{reboiler} + p_2 \times Q_{regen} + p_3 \times T_{reboiler}^2 + p_4 \times T_{reboiler} \times Q_{regen} + p_5 \times Q_{regen}^2 + 1.5 \quad (16)$$

$$NEP_{P_{Des}=1bar} = p_0 + p_1 \cdot T_{reboiler} + p_2 \cdot Q_{regen} + p_3 \cdot T_{reboiler}^2 + p_4 \cdot T_{reboiler} \cdot Q_{regen} + p_5 \cdot Q_{regen}^2 + p_6 \cdot T_{reboiler}^2 \cdot Q_{regen} + p_7 \cdot T_{reboiler} \cdot Q_{regen}^2 + p_8 \cdot Q_{regen}^3 + 1.5 \quad (17)$$

Table 7
Polynomial parameters for the calculation of *NEP* and NPL^{Tot} models.

Model	*NEP*		NPL^{Tot}
Parameter	P_{Des} = 1.5 bar	P_{Des} = 1 bar	-
p0	27.64	17.92	404.2
p1	−0.3967	−0.2589	−7.815
p2	−2.032	1.88	87.53
p3	0.001571	0.001257	0.03538
p4	0.03369	−0.00589	−0.4284
p5	0.00979	−0.5071	−24.07
p6	–	−4.76E-05	0.001619
p7	–	0.007714	0.1531
p8	–	−0.03619	0.9048

The equations are derived from a nomogram which accounts for power loss due to steam extraction and CO_2 compression at 110 bar in case of retrofit integration in a power plant. The last term of 1.5 in Eqs. 16 and 17 is added because according to Oexman (2011) the *NEP* calculations need to account for auxiliary power required for additional pumps and fans in the capture process and auxiliary power of additional cooling water pumps. These are not considered in the nomogram but they roughly account for an additional *NEP* of 1.5%-pts (Oexman, 2011).

In order to calculate R_{lost}, the total net power loss (NPL^{Tot}) is calculated from Eq. (18) which is also fitted from the same nomogram of Oexman (2011) . Table 7 shows the coefficients of the polynomial of Eq. (18).

$$NPL^{Tot} = p_0 + p_1 \cdot T_{reboiler} + p_2 \cdot Q_{regen} + p_3 \cdot T_{reboiler}^2 + p_4 \cdot T_{reboiler} \cdot Q_{regen} + p_5 \cdot Q_{regen}^2 + p_6 \cdot T_{reboiler}^2 \cdot Q_{regen} + p_7 \cdot T_{reboiler} \cdot Q_{regen}^2 + p_8 \cdot Q_{regen}^3 \quad (18)$$

Net electricity ($N_{elec}^{CO_2}$) in the presence of the capture unit is calculated as follows:

$$N_{elec}^{CO_2} = N_{elec} - NPL^{Tot} \quad (19)$$

where N_{elec} = 620 MW_e. The R_{lost} per year is calculated from Eq. (20) as follows:

$$R_{lost} = 1186.68 - 8700 \cdot C_{elec} \cdot N_{elec}^{CO_2} \quad (20)$$

where 1186.68 M€/yr corresponds to the revenue of the power plant without a capture unit for electricity price of C_{elec} = 220 €/MWh, assuming 8700 h/year (Eurostat, 2018).

4. Results and discussion

4.1. Operating results

The reboiler duty results for all solvents is shown in Fig. 4, with division of the energy terms of Q_{sens}, Q_{latent}, and Q_{rxn} according to Eq. (2). It becomes clear that the phase-change solvents MCA and MAPA/DEEA exhibit reboiler duties close to 2 GJ/ton CO_2. For MAPA/DEEA this is in line with the experimentally determined reboiler duty of Pinto et al. (2014a) who report 2.2–2.4 GJ/ton CO_2. Note that Fig. 4 reports the minimum reboiler duty values observed within a wide lean loading range. Our result is 2.1 GJ/ton CO_2 while results

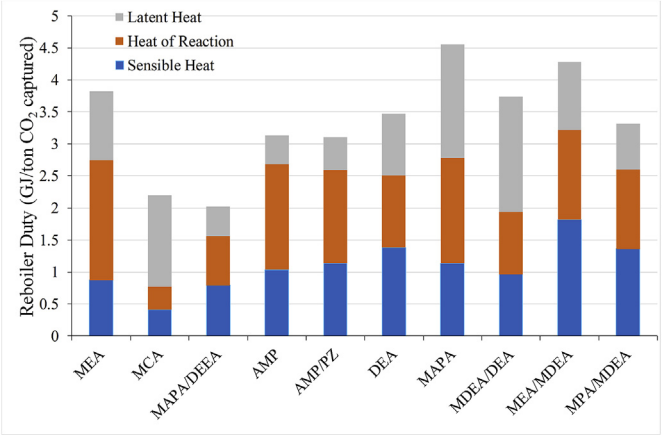

Fig. 4. Reboiler duties of investigated solvents.

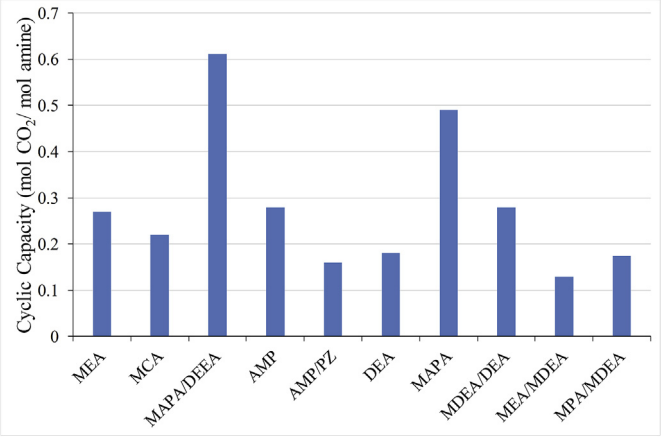

Fig. 5. Cyclic capacity where minimum reboiler duty is obtained.

up to 2.4 GJ/ton CO_2 were also calculated. Within a lean loading range of 0.19–0.24 the reboiler temperatures ranged between 87 and 96 °C, which are also in line with the temperatures of 93–103 °C reported by Pinto et al. (2014a). The difference is reasonable considering that the proposed model includes assumptions. It is also worth noting that the desorber pressure reported by Pinto et al. (2014a) is about 1.75 bar, whereas our results are for 1.5 bar. There are no specific data for MCA, but Zhang (2013) reports reboiler duties of 2–2.5 GJ/ton CO_2 for the mixture MCA/DMCA/AMP. Since MCA exhibits phase change the reboiler duty of 2.12 GJ/ton CO_2 reported in Fig. 4 is a reasonable value.

Fig. 5 illustrates the cyclic capacities where minimum reboiler duty is obtained. Cyclic capacity is an indirect indicator for CAPEX. Larger cyclic capacity enables reduction in the size of the absorption column. It is clear from Fig. 5 that MAPA/DEEA is the best option in this indicator, followed by MAPA. For these two solvents the large cyclic capacity is partly due to the high rich loading that can be obtained, in the sense that it is difficult to attain high cyclic capacity in solvents exhibiting low rich loadings. This is because in such a case the lean loading needs to be reduced significantly with detrimental effects on the reboiler duty.

Fig. 6 reports the calculated operating parameters of the solvents compared to MEA. Specifically, $T_{reboiler}$ (T_6) and T_{richin} (T_5) are very similar to those of MEA with expected, small differences particularly in phase-change solvents. Fig. 6 highlights the superiority of the phase-change solvent MAPA/DEEA considering the cyclic capacity and the ability of the solvent to capture a larger

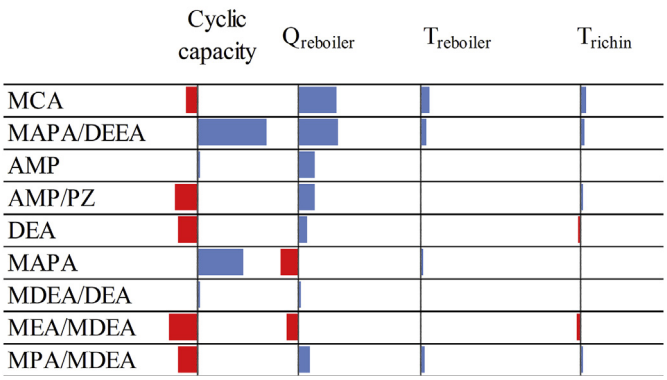

Fig. 6. Operating parameters with respect to MEA, blue bars pointing right indicate lower values than MEA, whereas red bars pointing left indicate higher values. Data are for the case of minimum reboiler duty. (For interpretation of the references to colour in this figure legend, the reader is referred to the Web version of this article.)

amount of CO_2 than MEA through a single pass. In terms of the regeneration energy, all solvents apart from MAPA and MEA/MDEA exhibit improved performance compared to MEA.

4.2. Technoeconomic evaluation

Table 8 provides indicative results from the performed simulations over a range of different cyclic capacities for all solvents. Reboiler temperature is reported as an average within the investigated cyclic capacity ranges, whereas the minimum values are reported for the remaining indicators. Notice that the lost power and revenue are reduced by 40–50% with phase change solvents compared to MEA.

Fig. 7 illustrates the *NEP* introduced in the operation of a power plant by the use of a solvent. In general, phase-change solvents exhibit much lower penalty values than the conventional solvents. For DMX, another phase-change solvent reported in literature, Dreillard et al. (2017) report 9.1 %-pts, whereas the *NEP* in Fig. 7 is 8.13 %-pts and 8.88 %-pts for MAPA/DEEA and MCA, respectively. The results in Fig. 7 correspond to the minimum reboiler duty values over the studied range of CO_2 loading. According to Liebenthal et al. (2013), MAPA/DEEA has been estimated to reach 5.9 %-pts for a reboiler duty of 2.4 GJ/ton CO_2 at reboiler temperature 88 °C and 4 bar pressure. Note that except for the desorber pressure, the reboiler temperature and duty are within the same range as in the case of 1.75 bar pressure reported previously. By the same token, using the same results for MAPA/DEEA obtained in the simulations and changing the pressure to 4 bar, the estimated *NEP* is 6 %-pts. Although this is a rough approximation, it is another indication that the results are verified for MAPA/DEEA.

Fig. 8 illustrates several solvent parameters associated with process performance. It is desirable to use solvents exhibiting low reboiler duty and solvent flowrate as well as high cyclic capacity. The different data points for each solvent refer to different lean loading ranges in which the solvents were investigated. Fig. 8 illustrates the relative performance of the solvents; hence the triangle axes represent scaled, not absolute values. Phase-change solvents exhibit considerably lower reboiler duties than the conventional solvents. However, the cyclic capacities and the mass flowrates required by the phase-change solvents are in general equivalent to those of the conventional solvents. Considering that the lower and upper limits observed for phase-change solvents in the solvent flowrate axis are approximately from 35% to 90% and 10%–65% in the cyclic capacity axis, all solvents are approximately spread within this area. Furthermore, MAPA/DEEA performs slightly better than MCA in terms of cyclic capacity and solvent flowrate. It is worth noting that MAPA performs well only in terms of solvent flowrate. However, when MAPA is used in a mixture with DEEA (MAPA/DEEA) the reboiler duty drops significantly.

The reboiler duty is not the best indicator to evaluate a solvent. Net efficiency penalty considers both the reboiler temperature and desorber pressure hence it provides a much more inclusive evaluation of the solvent performance. This becomes clear already from Figs. 4 and 7, where MDEA/DEA exhibits a significantly lower reboiler duty than MEA/MDEA, but their net efficiency penalty values are very similar. Since the desorber pressure is the same, the similar net efficiency penalty is because the reboiler temperature of MEA/MDEA is lower than MDEA/DEA. Fig. 9 therefore illustrates the net efficiency penalty with respect to solvent flowrate and cyclic capacity. In this case the difference between MAPA/DEEA and MCA becomes clearer. The lower performance of MCA is because the calculations were performed at desorber pressure of 1 bar due to availability of data, whereas all other solvents were estimated at 1.5 bar. Note that the cyclic capacity of all solvents is slightly different in Fig. 9, compared to Fig. 8, because the values in the axes

Table 8
Representative results for the investigated solvents in operating and performance indicators.

Solvent	$T_{reboiler}$ (average) [K]	Cyclic capacity (range)	*NEP* (min) [%-pts]	NPL^{Tot} (min) [MW_{el}]	R_{lost} (min) [M€/yr]
MEA	385.9	[0.13,0.27]	11.43	156.2	299.0
MCA	361.9	[0.13,0.28]	8.88	82.7	158.3
MAPA/DEEA	364.9	[0.53,0.64]	8.13	76.6	146.6
AMP	370.7	[0.20,0.45]	9.39	107.9	206.5
AMP/PZ	379.6	[0.09,0.26]	9.56	110.9	212.2
DEA	379.7	[0.09,0.32]	10.14	124.7	238.7
MAPA	385.6	[0.39,0.69]	12.51	186.1	356.1
MDEA/DEA	385.2	[0.08,0.28]	11.31	153.2	293.2
MEA/MDEA	379.4	[0.07,0.22]	11.40	156.0	298.6
MPA/MDEA	375.1	[0.14,0.29]	9.69	114.5	219.1

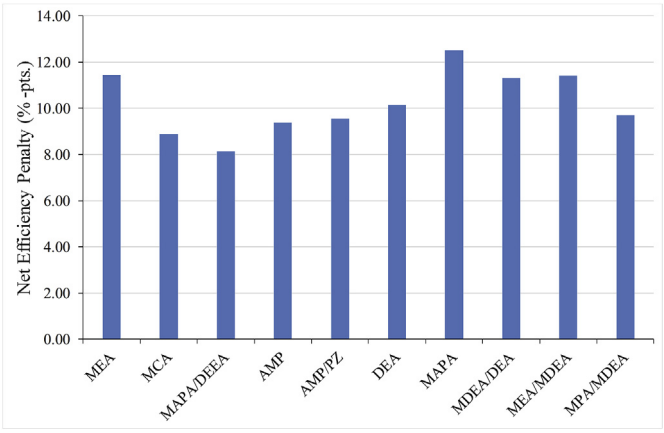

Fig. 7. Net efficiency penalty of investigated solvents.

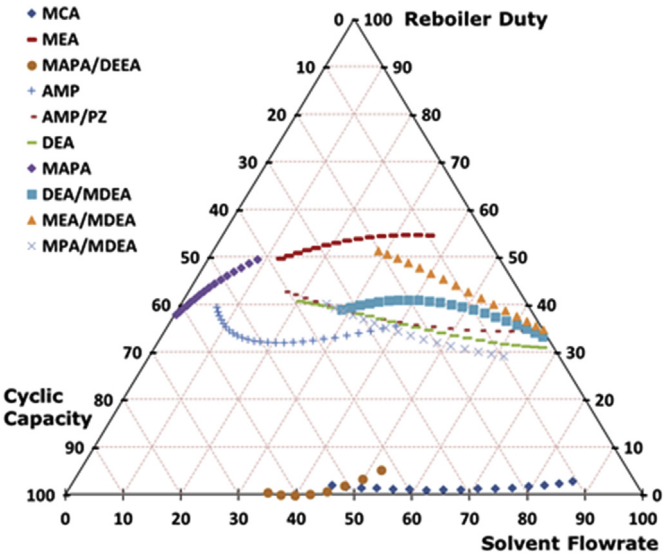

Fig. 8. Comparative assessment of reboiler duty, solvent flowrate and cyclic capacity.

are relative and not absolute (i.e. the use of the net efficiency penalty instead of reboiler duty changes the scaling). However, the overall trend remains the same. The difference in net efficiency penalty also makes the lower cyclic capacity of MCA clearer.

The results of Fig. 9 become more practical in Fig. 10, where the net efficiency penalty is translated to lost revenue from parasitic electricity and the solvent flowrate to solvent purchase cost. The

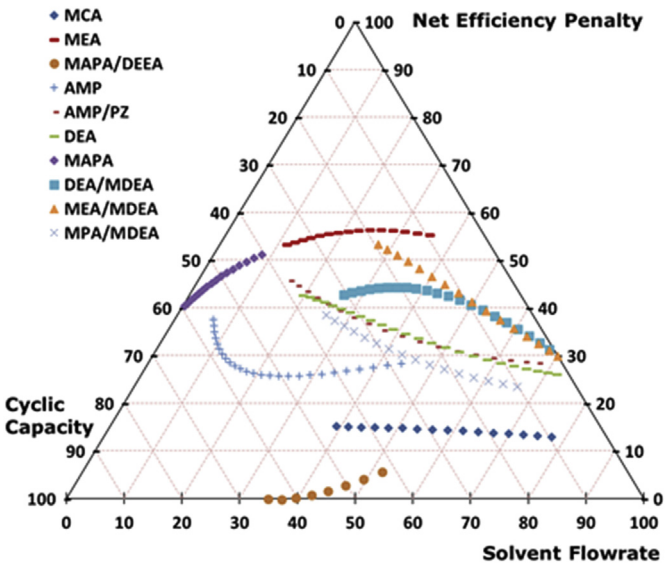

Fig. 9. Comparative assessment of net efficiency penalty, solvent flowrate and cyclic capacity.

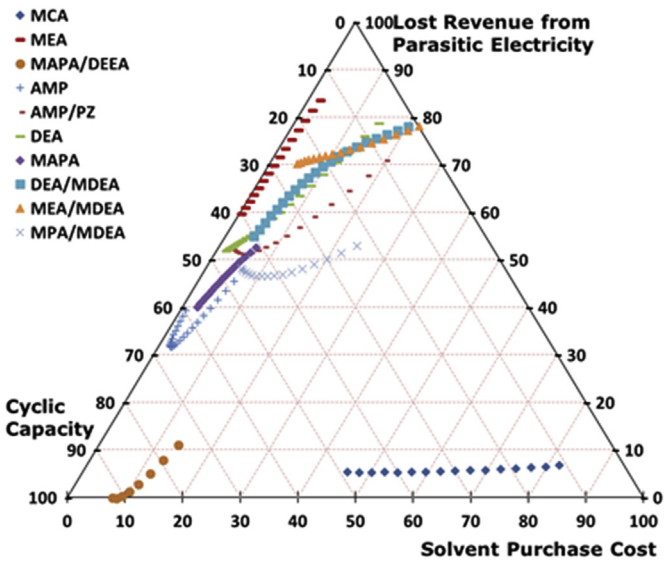

Fig. 10. Comparative assessment of lost revenue from parasitic electricity, solvent purchase cost and cyclic capacity.

lost revenue from parasitic electricity corresponds to revenue that would otherwise be made if all the power plant electricity was sold to consumers. So instead of energy penalty values, we include directly the total net power loss of the plant. The solvent purchase cost further introduces significant changes in the rank-ordering of the solvents because by considering the solvent flowrate as a criterion we practically assume that the solvent prices are the same. The price of MCA is 7 times higher than the price of MAPA/DEEA and this is clearly reflected in Fig. 10. In this respect MAPA/DEEA seems to be the best option. A different aspect, which is pronounced in Fig. 10, is that the lost revenue for MCA has very low sensitivity in changes in cyclic capacity and solvent costs. On the other hand, most solvents are very sensitive to changes in cyclic capacity. NPL^{Tot} in Eq. (18) is used to calculate the lost revenue and is very non-linear with respect to both the reboiler temperature and the reboiler duty. Considering this equation and based on the performed simulations, this reduced sensitivity of MCA is due to the low sensitivity of the reboiler temperature and duty to changes in cyclic capacity and solvent flowrate. The other solvents are much more sensitive in such changes and this is propagated through the NPL^{Tot} model to the calculation of the lost revenue.

4.3. Sustainability, degradation and corrosion

From the reported results it is possible to perform a qualitative, preliminary assessment of solvent environmental, health and safety impacts. An important feature observed in Table 8 is the lower reboiler temperature for several solvents and especially for the phase-change solvents, which is over 20 K lower than that of MEA. Reboiler temperatures of 363 K or lower, as those of MCA and MAPA/DEEA, could enable the exploitation of waste heat sources from the emitting plants. This has significant environmental advantages as the use of fossil-based steam in the regeneration may be reduced or eliminated. The lower operating temperatures may further reduce volatility losses as well as thermally induced degradation of the solvent. For amines with similar boiling point like MEA and AMP, the lower volatility losses expected for AMP would improve indices like chronic toxicity (Shavalieva et al., 2019; Papadopoulos et al., 2020), hence supporting a healthier working environment and lower air-mediated environmental impacts. The reduction of thermal degradation is desirable as the formation of carcinogenic products such as nitrosamines is reduced at lower temperatures (Yu et al., 2017). However, nitrosamines tend to accumulate at low temperatures as they are soluble in water (Shavalieva et al., 2019), whereas they may only be destroyed at high desorption temperatures (Yu et al., 2017). Papadokonstantakis et al. (2015) performed life-cycle (LCA) and environmental, health and safety (EHS) hazard assessment of MEA, DEA and AMP considering different capture process configurations. They considered thermal and oxidative degradation of the amines as well as landfilling or waste-water treatment scenarios for the reclaimed solvent. AMP was found to exhibit the lowest life-cycle impacts among the three, due to its lowest reboiler duty. The latter is also verified here, whereas AMP has the lowest reboiler duty among all non-phase-change solvents, as shown in Fig. 4. AMP was also found to exhibit the lowest EHS impacts among MEA and DEA due to its higher stability, lower toxicity and process circulating rates. Expressed as solvent flowrate here, the lower circulating rate is verified for AMP, as shown in Figs. 8 and 9. It is in fact observed at higher cyclic capacity than for all other non-phase-change solvents, and is only overcome by MAPA. Shavalieva et al. (2019) performed a comparative, cradle-to-gate LCA and EHS analysis of MCA and MEA. The life-cycle impact of MCA was found to be lower than MEA, with reboiler steam being the main contributor. Due to its much lower reboiler duty than MEA, it is likely that MAPA/DEEA will also exhibit a lower life-cycle impact. In terms of health and safety, the MCA performance was found similar to or better than MEA, whereas the formation of nitrosamines was found to be the most important contributor to environmental impacts. Life-cycle and EHS investigations have not been performed for MAPA/DEEA.

With respect to degradation and corrosion, several of the solvents are discussed and rank-ordered based on quantitative data available in literature sources. The mixtures of non-phase-change solvents are not presented here due to their much more complex dependence on conditions and compositions than the individual solvents (Mazari et al., 2014), but also due to our focus on phase-change solvents. Lepaumier et al. (2009) find that the ranking of some of the investigated amines in terms of thermal degradation rate in the absence of gases decreases in the order DEA > MEA > MDEA > AMP. MPA is very similar to MEA in terms of structure (different by one methanediyl group) hence it could be assumed that it performs similarly. In absolute values the thermal degradation rates are very small compared to the much higher rates of thermal degradation in the presence of CO_2. In this case, the ranking in decreasing order is DEA > MEA > AMP > MDEA (Lepaumier et al., 2009). MCA performs worse than both MEA and AMP in the presence of CO_2 (Zhang, 2014). MAPA could be placed after MEA, as its thermal degradation is slightly lower than MEA (Shavalieva et al., 2020). DEEA is also more resilient to thermal degradation than MEA (Gao et al., 2014). In this respect, the MAPA/DEEA mixture is likely to exhibit lower thermal degradation than MEA. For oxidative degradation, the ranking in decreasing order is DEA > MEA > MDEA > AMP (Lepaumier et al., 2009). According to literature studies, the oxidative degradation rate of MAPA is 3–10 times higher than MEA (Voice et al., 2013). MCA again performs worse than both MEA and AMP (Zhang, 2014). Finally, PZ is much more resilient in both thermal and oxidative degradation than MEA and AMP (Freeman et al., 2010).

With respect to corrosion, Pinto et al. (2014a) note that in pilot plant experiments with MAPA/DEEA some corrosion is observed, with the iron content being at the same levels as a corresponding conventional MEA process. The metal concentrations are stabilized after 3 weeks of operation. Gunasekaran et al. (2017) perform a corrosivity analysis of several solvents and find that the corrosivity of carbon steel in single amine systems saturated with CO_2 at 80 °C decreases in the following order: MEA > AMP > DEA > PZ > MDEA. MAPA/DEEA will therefore rank similarly to MEA. MPA has a very similar structure to MEA hence a similar behavior may be expected compared to the other amines reported here. No data are available regarding the corrosivity behavior of MCA. It should be noted that corrosion increases with temperature (Gunasekaran et al., 2017), hence the lower regeneration temperature of MCA is expected to be an advantage compared to the other amines.

5. Conclusions

This work develops and implements a shortcut model for the efficient screening and assessment of phase-change solvents based on process behavior. The vast majority of published shortcut or rigorous CO_2 capture process models address only conventional solvents that exhibit VLE instead of VLLE behavior. Shortcut methods are much faster than rigorous models and permit the identification of important, process-related features, highlighting both the economic and energetic performance of solvents for absorption-based CO_2 capture processes. It is worth noting that shortcut models are not meant to replace the rigorous models needed to determine process characteristics. They should be used to enable solvent evaluation and comparison based on criteria that reflect their impact on the process where they are used. Such an approach allows the fast identification of poorly performing

options and their elimination from further investigation in rigorous process models and experiments. At the same time, effort and resources may be invested on few, promising solvents. In this respect, process-based solvent assessment, considering multiple different indicators simultaneously, improves the reliability of the decision-making compared to selecting solvents based purely on physical or chemical properties. As shown in the results of the case studies, the use of different criteria has an impact on the relative performance of the solvents. Solvent costs should be accounted for in the decision-making as the employed solvent quantities are not negligible. Furthermore, differences in reboiler temperatures may result in similar net efficiency penalties, despite differences in reboiler duties.

Phase-change solvents require low regeneration energy and hence they are characterized by superiority in energetic aspects. The main points identified in this work are summarized as follows:

- Phase-change solvents MCA and MAPA/DEEA exhibit superior performance in terms of both reboiler duty and net efficiency energy penalty points, when integrated with a power plant. The reboiler duty is 2.0–2.3 GJ/ton CO_2 captured, much lower than the 3.1 GJ/ton CO_2 obtained in the best case for the conventional mixture of AMP/PZ.
- In addition to the above performance indicators, cyclic capacity, solvent mass flowrate, solvent purchase cost and lost revenue from parasitic electricity are also considered. The two latter indicators directly associate the solvent performance with operating process costs, providing a clearer overview regarding the performance of the investigated solvents. Although cyclic capacity is associated with absorber and desorber capital costs, most of the results pertain to operating process evaluation. Clearly, indicators related to capital costs would also be needed as they may be a decisive factor in many cases. Note that a detailed analysis including both operating and capital expenditures for the DMX™ phase change solvent showed that the cost per ton of CO_2 capture is much lower compared to MEA (Gomez et al., 2014). This indicates that the addition of equipment (decanter) in phase-change processes is likely to have a small effect on overall costs compared to conventional systems.
- The selected phase-change solvents exhibit better performance compared to conventional solvents. MAPA/DEEA performs better than MCA in terms of solvent purchase cost, while the performance of both solvents is similar in terms of lost revenue from parasitic electricity losses.
- MCA is 44%, and 47% better than MEA in reboiler duty and lost revenue due to parasitic losses, while it is also 2.9 %-pts lower in terms of net efficiency penalty. MAPA/DEEA is 45%, 50% and 3.3 %-pts better than MEA in the corresponding indicators.
- The desorption temperature of 363 K or lower observed in phase-change solvents may facilitate the use of waste heat from the emitting plant with beneficial environmental effects. The life-cycle impact of MCA was found to be lower than MEA by Shavalieva et al. (2019), with reboiler steam being the main contributor. The equivalent low energetic requirements of MAPA/DEEA indicate that this solvent may also exhibit low life-cycle impacts, although a detailed analysis is needed to this end.
- In terms of EHS impacts, the formation of nitrosamines is very important. Nitrosamines are reduced at lower desorption temperatures, as those observed in phase-change solvents, but they tend to accumulate in the system as they may only be destroyed at higher temperatures (Yu et al., 2017).
- In terms of degradation, AMP and MDEA are more resilient than MEA in both oxidative and thermal degradation, whereas MCA performs worse than MEA in both cases. MAPA/DEEA is more resilient than MEA in thermal degradation, but MAPA is less resilient than MEA in oxidative degradation. In terms of corrosion, MDEA is a very good option, better than MEA, whereas MAPA/DEEA ranks similarly to MEA. Although data are not available for MCA, the much lower operating temperature of the process is clearly advantageous compared to the other amines.

CRediT authorship contribution statement

Theodoros Zarogiannis: Conceptualization, Methodology, Software, Writing - original draft, Writing - review & editing, Visualization. **Athanasios I. Papadopoulos:** Conceptualization, Methodology, Supervision, Writing - original draft, Writing - review & editing, Project administration, Funding acquisition. **Panos Seferlis:** Conceptualization, Methodology, Supervision, Writing - original draft, Writing - review & editing, Project administration, Funding acquisition.

Declaration of competing interest

The authors declare that they have no known competing financial interests or personal relationships that could have appeared to influence the work reported in this paper.

Acknowledgements

This project has received funding from the European Union's Horizon 2020 research and innovation program under the grant agreement 727503 - ROLINCAP – H2020-LCE-2016-2017/H2020-LCE-2016-RES–CCS–RIA.

Nomenclature

AMP	2-amino-2-methyl-1-propanol
C_{sol}	Solvent purchase cost ($/gr)
DEA	Diethanolamine
DEEA	2-(diethylamino)ethanol
EHS	Environmental, health and safety assessment
$K_{Dc,i}$	Equilibrium constant for component i
LCA	Life cycle assessment
LLPS	Liquid-liquid phase separation temperature
m_{am}	Molar flowrate of amines per ton of CO_2 product (mol/t CO_2 product)
MAPA	3-(methylamino)propylamine
MCA	Methyl-cyclohexylamine
MDEA	Methyldiethanolamine
MEA	Monoethanolamine
MPA	3-amino-1-propanol
NEP	Net efficiency penalty (percentage points)
P^*_{CO2}	Partial pressure of CO_2 (kPa)
PZ	Piperazine
Q_{latent}	Latent heat (kJ/ton CO_2)
Q_{regen}	Regeneration duty
Q_{rxn}	Heat of reaction (kJ/ton CO_2)
Q_{sens}	Sensible heat (kJ/ton CO_2)
R	Universal gas constant ($8.314 \cdot 10^{-3}$ kJ/mol K)
R_{lost}	Lost revenue from parasitic electricity (M€/yr)
T	Temperature (K)
VLE	Vapor-liquid equilibrium
VLLE	Vapor-liquid-liquid equilibrium
x	Liquid fraction
y	Vapor fraction

Indices

i	Component

$_L$	Liquid phase
$_V$	Vapor phase

Greek symbols

a	CO_2 loading (mol CO_2/mol amine)
Δa	Cyclic capacity (mol CO_2/mol amine)

Appendix A. Supplementary data

Supplementary data to this article can be found online at https://doi.org/10.1016/j.jclepro.2020.122764.

References

Achenie, L., Venkatasubramanian, V., Gani, R. (Eds.), 2002. Computer Aided Molecular Design: Theory and Practice. Elsevier.

Arshad, M.W., 2014. Measuring and Thermodynamic Modeling of De-mixing CO_2 Capture Systems. PhD Thesis. Center for Energy Resources Engineering. Technical University of Denmark.

Bruder, P., Grimstvedt, A., Mejdell, T., Svendsen, H.F., 2011. CO_2 capture into aqueous solutions of piperazine activated 2-amino-2-methyl-1-propanol. Chem. Eng. Sci. 66 (23), 6193–6198.

Bruder, P., Lauritsen, K.G., Mejdell, T., Svendsen, H.F., 2012. CO_2 capture into aqueous solutions of 3-methylaminopropylamine activated dimethyl-monoethanolamine. Chem. Eng. Sci. 75, 28–37.

Bui, M., Adjiman, C.S., Bardow, A., Anthony, E.J., Boston, A., Brown, S., Fennell, P.S., Fuss, S., Galindo, A., Hackett, L.A., Hallett, J.P., Herzog, H.J., Jackson, G., Kemper, J., Krevor, S., Maitland, G.C., Matuszewski, M., Metcalfe, I.S., Petit, C., Puxty, G., Reimer, J., Reiner, D.M., Rubin, E.S., Scott, S.A., Shah, N., Smit, B., Trusler, J.P.M., Webley, P., Wilcoxx, J., Mac Dowell, N., 2018. Carbon capture and storage (CCS): the way forward. Energy Environ. Sci. 11 (5), 1062–1176.

Chapman, W.G., Gubbins, K.E., Jackson, G., Radosz, M., 1989. SAFT: equation-of-state solution model for associating fluids. Fluid Phase Equil. 52, 31–38.

Chapman, W.G., Gubbins, K.E., Jackson, G., Radosz, M., 1990. New reference equation of state for associating liquids. Ind. Eng. Chem. Res. 29 (8), 1709–1721.

Chem-Space, 2018. URL chem-space.Com [WWW Document].

Chremos, A., Forte, E., Papaioannou, V., Galindo, A., Jackson, G., Adjiman, C.S., 2016. Modelling the phase and chemical equilibria of aqueous solutions of alkanolamines and carbon dioxide using the SAFT-γ SW group contribution approach. Fluid Phase Equil. 407, 280–297.

Dreillard, M., Broutin, P., Briot, P., Huard, T., Lettat, A., 2017. Application of the DMX^{TM} CO_2 capture process in steel industry. Energy Procedia 114, 2573–2589. https://doi.org/10.1016/J.EGYPRO.2017.03.1415.

Dufal, S., Papaioannou, V., Sadeqzadeh, M., Pogiatzis, T., Chremos, A., Adjiman, C.S., Jackson, G., Galindo, A., 2014. Prediction of thermodynamic properties and phase behavior of fluids and mixtures with the SAFT-γ Mie group-contribution equation of state. J. Chem. Eng. Data 59 (10), 3272–3288.

Dufal, S., Lafitte, T., Haslam, A.J., Galindo, A., Clark, G.N., Vega, C., Jackson, G., 2015. The A in SAFT: developing the contribution of association to the Helmholtz free energy within a Wertheim TPT1 treatment of generic Mie fluids. Mol. Phys. 113 (9-10), 948–984.

Eurostat, 2018. Electricity price statistics explained [WWW Document]. URL https://ec.europa.eu/eurostat/statistics-explained/index.php/Electricity_price_statistics. .

Freeman, S.A., Davis, J., Rochelle, G.T., 2010. Degradation of aqueous piperazine in carbon dioxide capture. Int. J. Greenh. Gas Contr. 4 (5), 756–761.

Gao, H., Rongwong, W., Peng, C., Liang, Z., Fu, K., Idem, R., Tontiwachwuthikul, P., 2014. Thermal and oxidative degradation of aqueous N, N-Diethylethanolamine (DEEA) at stripping conditions for CO_2 capture. Energy Procedia 63, 1911–1918.

Gil-Villegas, A., Galindo, A., Whitehead, P.J., Mills, S.J., Jackson, G., Burgess, A.N., 1997. Statistical associating fluid theory for chain molecules with attractive potentials of variable range. J. Chem. Phys. 106 (10), 4168–4186.

Gomez, A., Briot, P., Raynal, L., Broutin, P., Gimenez, M., Soazic, M., Cessat, P., Saysset, S., 2014. ACACIA Project – development of a post-combustion CO_2 capture process. Case of the DMX$_{TM}$ Process. Oil Gas Sci. Techol. – Rev. IFP Energies Nouv 69, 1121–1129.

gSAFT, 2018. Process systems enterprise ltd. URL. www.psenterprise.com/products/gsaft.

Gunasekaran, P., Veawab, A., Aroonwilas, A., 2017. Corrosivity of amine-based absorbents for CO_2 capture. Energy Procedia 114, 2047–2054.

Kim, H., Hwang, S.J., Lee, K.S., 2015. Novel shortcut estimation method for regeneration energy of amine solvents in an absorption-based carbon capture process. Environ. Sci. Technol. 49, 1478–1485.

Kremser, A., 1930. A theoretical analysis of absorption process. Natl. Petrol. News 22, 43–49.

Lepaumier, H., Picq, D., Carrette, P.L., 2009. New amines for CO_2 capture. I. Mechanisms of amine degradation in the presence of CO_2. Ind. Eng. Chem. Res. 48 (20), 9061–9067.

Liebenthal, U., Di, D., Pinto, D., Monteiro, J.G.M.S., Svendsen, H.F., Kather, A., 2013. Overall process analysis and optimisation for CO_2 Capture from coal fired power plants based on phase change solvents forming two liquid phases. In: Energy Procedia, pp. 1844–1854.

Lucia, A., Anirban, R., Sorin, M., 2010. Energy efficient synthesis and design for carbone capture. In: In Proceedings of Distillation Absorption 2010, pp. 97–102. In: http://folk.ntnu.no/skoge/prost/proceedings/distillation10/DA2010%20Conference%20Proceedings/2.%20Carbon%20Dioxide%20Capture/OR06%20Lucia%20Energy%20Efficient%20Synthesis%20and%20Design.pdf.

Mac Dowell, N., Llovell, F., Adjiman, C.S., Jackson, G., Galindo, A., 2009. Modeling the fluid phase behavior of carbon dioxide in aqueous solutions of monoethanolamine using transferable parameters with the SAFT-VR approach. Ind. Eng. Chem. Res. 49 (4), 1883–1899.

Mazari, S.A., Ali, B.S., Jan, B.M., Saeed, I.M., 2014. Degradation study of piperazine, its blends and structural analogs for CO_2 capture: a review. Int. J. Greenh. Gas Contr. 31, 214–228.

Notz, R., Tönnies, I., Mangalapally, H.P., Hoch, S., Hasse, H., 2011. A short-cut method for assessing absorbents for post-combustion carbon dioxide capture. Int. J. Greenh. Gas Control 5, 413–421.

Oexman, J., 2011. Post- combustion CO_2 capture: energetic evaluation of chemical absorption processes in coal–fired steam power plants. Technischen Universität Hamburg-Harburg.

Oyenekan, B.A., 2007. Modeling of Strippers for CO_2 Capture by Aqueous Amines. University of Texas at Austin. https://repositories.lib.utexas.edu/handle/2152/3134. PhD Thesis.

Papadokonstantakis, Stavros, Badr, S., Hungerbühler, K., Papadopoulos, A.I., Damartzis, T., Seferlis, P., Forte, E., Chremos, A., Galindo, A., Jackson, G., Adjiman, C., 2015. Toward sustainable solvent-based postcombustion CO_2 capture: from molecules to conceptual flowsheet design. In: Computer Aided Chemical Engineering, vol. 36. Elsevier, pp. 279–310.

Papadopoulos, A.I., Seferlis, P., 2017a. Process Systems and Materials for CO_2 Capture: Modelling, Design, Control and Integration. John Wiley & Sons, Chichester.

Papadopoulos, A.I., Zarogiannis, T., Seferlis, P., 2017b. Computer-aided molecular design of CO_2 capture solvents and mixtures. In: Process Systems and Materials for CO_2 Capture. John Wiley & Sons, Ltd, Chichester, UK, pp. 173–201. https://doi.org/10.1002/9781119106418.ch7.

Papadopoulos, A.I., Tsivintzelis, I., Linke, P., Seferlis, P., 2018. Computer-aided molecular deisgn:fundamentals, methods and applications. In: Reedijk, J. (Ed.), Elsevier Reference Module in Chemistry, Molecular Sciences and Chemical Engineering. Elsevier, Waltham, MA. https://doi.org/10.1016/B978-0-12-409547-2.14342-2.

Papadopoulos, A.I., Tzirakis, F., Tsivintzelis, I., Seferlis, P., 2019. Phase-change solvents for post-combustion CO_2 capture- A detailed review. Ind. Eng. Chem. Res. 58, 5088–5111.

Papadopoulos, A.I., Shavalieva, G., Papadokonstantakis, S., Seferlis, P., Perdomo, F.A., Galindo, A., Jackson, G., Adjiman, C.S., 2020. An approach for simultaneous computer-aided molecular design with holistic sustainability assessment: application to phase-change CO_2 capture solvents. Comput. Chem. Eng. 135, 106769. https://doi.org/10.1016/j.compchemeng.2020.106769.

Papaioannou, V., Lafitte, T., Avendano, C., Adjiman, C.S., Jackson, G., Müller, E.A., Galindo, A., 2014. Group contribution methodology based on the statistical associating fluid theory for heteronuclear molecules formed from Mie segments. The Journal of Chemical physics, 140(5), 054107.

Papaioannou, V., Calado, F., Lafitte, T., Dufal, S., Sadeqzadeh, M., Jackson, G., Adjiman, C.S., Galindo, A., 2016. Application of the SAFT-γ Mie group contribution equation of state to fluids of relevance to the oil and gas industry. Fluid Phase Equil. 416, 104–119.

Perdomo, F.A., Khalit, S.H., Adjiman, C.A., Galindo, A., Jackson, G., 2019. Prediction of Thermodynamic Properties and Phase Behaviour of Complex Aqueous Solutions of Amines. In preparation.

Pinto, D.D.D., Knuutila, H., Fytianos, G., Haugen, G., Mejdell, T., Svendsen, H.F., 2014a. CO_2 post combustion capture with a phase change solvent. Pilot plant campaign. Int. J. Greenh. Gas Control 31, 153–164.

Pinto, D.D.D., Zaidy, S.A.H., Hartono, A., Svendsen, H.F., 2014b. Evaluation of a phase change solvent for CO_2 capture: absorption and desorption tests. Int. J. Greenh. Gas Control 28, 318–327.

Raynal, L., Alix, P., Bouillon, P.A., Gomez, A., Le Febvre De Nailly, M., Jacquin, M., Kittel, J., Di Lella, A., Mougin, P., Trapy, J., 2011a. The DMX^{TM} process: an original solution for lowering the cost of post-combustion carbon capture. Energy Procedia 779–786.

Raynal, L., Bouillon, P.A., Gomez, A., Broutin, P., 2011b. From MEA to demixing solvents and future steps, a roadmap for lowering the cost of post-combustion carbon capture. Chem. Eng. J. 171, 742–752.

Raynal, L., Briot, P., Dreillard, M., Broutin, P., Mangiaracina, A., Drioli, B.S., Politi, M., La Marca, C., Mertens, J., Thielens, M.L., Laborie, G., Normand, L., 2014. Evaluation of the DMX process for industrial pilot demonstration - methodology and results. In: Energy Procedia, pp. 6298–6309.

Reddick, C., Sorin, M., Rheault, F., 2014. Energy savings in CO_2 (carbon dioxide) capture using ejectors for waste heat upgrading. Energy 65, 200–208.

Rochelle, G., Chen, E., Freeman, S., Van Wagener, D., Xu, Q., Voice, A., 2011. Aqueous piperazine as the new standard for CO_2 capture technology. Chem. Eng. J. 171, 725–733.

Rodriguez, J., Mac Dowell, N., Llovell, F., Adjiman, C.S., Jackson, G., Galindo, A., 2012. Modelling the fluid phase behaviour of aqueous mixtures of multifunctional alkanolamines and carbon dioxide using transferable parameters with the SAFT-VR approach. Mol. Phys. 110 (11-12), 1325–1348.

Shavalieva, G., Papadokonstantakis, S., Kazepidis, P., Papadopoulos, A.I., Seferlis, P.,

2019. Sustainability analysis of phase-change solvents for post-combustion CO_2 capture. Chemical Engineering Transactions 76, 1045–1050.
Shavalieva, G., Kazepidis, P., Papadopoulos, A.I., Seferlis, P., Papadokonstantakis, S., 2020. Environmental, health and safety assessment of post-combustion CO_2 capture processes with phase-change solvents. Submitted for Publication.
Tan, Y., 2010. Study of CO2 -Absorption into Thermomorphic Lipophilic Amine Solvents. PhD Thesis, TU Dortmund. https://eldorado.tu-dortmund.de/bitstream/2003/27427/2/Dissertation -Tan_Rev04.pdf.
Tock, L., Maréchal, F., 2014. Process design optimization strategy to develop energy and cost correlations of CO_2 capture processes. Comput. Chem. Eng. 61, 51–58.
Tzirakis, F., Tsivintzelis, I., Papadopoulos, A.I., Seferlis, P., 2019a. Experimental measurement of vapour-liquid-liquid equilibria of phase-change solvents. In: The 26th Thermodynamics Conference. Punta Umbría, Spain.
Tzirakis, F., Tsivintzelis, I., Papadopoulos, A.I., Seferlis, P., 2019b. Experimental measurement and assessment of equilibrium behaviour for phase change solvents used in CO_2 capture. Chem. Eng. Sci. 199, 20–27.
Voice, A.K., Vevelstad, S.J., Chen, X., Nguyen, T., Rochelle, G.T., 2013. Aqueous 3-(methylamino)propylamine for CO_2 capture. Int. J. Greenh. Gas Contr 15, 70–77.
Yu, K., Mitch, W.A., Dai, N., 2017. Nitrosamines and nitramines in amine-based carbon dioxide capture systems: fundamentals, engineering implications, and knowledge gaps. Environ. Sci. Technol. 51 (20), 11522–11536.
Zhang, J., 2014. Study on CO_2 Capture Using Thermomorphic Biphasic Solvents with Energy Efficient Regeneration. PhD Thesis. Unversity of Dortmund.
Zhang, J., Misch, R., Tan, Y., Agar, D.W., 2011. Novel thermomorphic biphasic amine solvents for CO_2 absorption and low-temperature extractive regeneration. Chem. Eng. Technol. 34, 1481–1489.
Zhang, J., Qiao, Y., Wang, W., Misch, R., Hussain, K., Agar, D.W., 2013. Development of an energy-efficient CO_2 capture process using thermomorphic biphasic solvents. In: Energy Procedia. Elsevier, pp. 1254–1261.